difference; f, dimensionless distribution function; f^0, local Maxwellian distribution function; **c** and **u**, reduced velocities of the molecules and the gas, respectively; $\delta = \sqrt{\pi}a/2\lambda$, reciprocal Knudsen number; and G, reduced flow rate of gas through the pore mouth. Subscripts: e, saturated vapor; a, gas in the infinite vessel with which the pore is connected; x and y, longitudinal and transverse components.

LITERATURE CITED

1. T. Soga, Phys. Fluids, No. 25 (11) (1982).
2. T. Soga and Y. Osaki, Trans. Jpn. Soc. Aero. Sci., 26, No. 74, 187-197 (1984).
3. N. V. Pavlyukevich, G. E. Gorelik, V. V. Levdanskii, et al., Physical Kinetics and Transport Processes in the Presence of Phase Transitions [in Russian], Minsk (1980).
4. F. M. Sharipov and T. V. Shchepetkina, in: Molecular Physics of Nonequilibrium Systems [in Russian], Novosibirsk (1984), pp. 15-20.
5. P. Gajewski and A. Wisniewski, Bull. Acad. Pol. Sci. Ser. Sci. Tech., 26, No. 5, 513-520 (1978).
6. P. L. Bhatnagar, E. P. Gross, and M. A. Kroock, Phys. Rev., 94, No. 3, 511-520 (1954).
7. L. V. Kantorovich and V. I. Krylov, Approximate Methods of Higher Analysis [in Rusaian], Moscow–Leningrad (1952).

INVESTIGATION OF VAPOR PHASE DYNAMICS IN THE FILM BOILING OF NITROGEN IN A CENTRIFUGAL FORCE FIELD

N. M. Levchenko and I. M. Kolod'ko

UDC 536.423

The wavelength and the bubble separation diameter and frequency have been measured for the film boiling of liquid nitrogen on a thin horizontal wire at acceleration loads $\eta \leq 375$. A description of the process is given. The results obtained are compared with the available experimental and theoretical data.

The widespread use of cryogenic fluids in the national economy requires a comprehensive study of the question of heat transfer in relation to various regime parameters (pressure, subcooling, acceleration load). In order to calculate the unsteady processes associated with the chilling of cryogenic devices in a centrifugal force field it is important to have information on the film boiling regime and, in particular, the vapor phase dynamics.

A visual study of the film boiling of nitrogen at various pressures, subcoolings and cylindrical heater dimensions was carried out under conditions of normal gravity in [1]. The effect of various parameters (heat flux, heater diameter, acceleration load, etc.) on the thermal and hydrodynamic characteristics of the film boiling process was considered for noncryogenic fluids in [2, 3]. Experimental data on the vapor phase dynamics associated with the film boiling of cryogenic fluids in a centrifugal force field, i.e., under the combined influence of acceleration load η, liquid subcooling Φ, and pressure P, are still lacking.

This investigation of the film boiling of nitrogen was carried out on the apparatus described in [4] (centrifuge with vertical axis of rotation) on the acceleration load interval $1 \leq \eta \leq 375$ and the heat flux interval $q_{cr2} \leq q \leq 4q_{cr1}$. As the heat-transfer surface we used a Nichrome wire $2.2 \cdot 10^{-4}$ m in diameter and $3.8 \cdot 10^{-3}$ m long arranged at right angles to the centrifugal acceleration vector and the axis of rotation. The heat-transfer surface was not specially cleaned after heating at heat fluxes up to 3-4 times greater than q_{cr1}.

At the level of the heat-transfer surface the pressure and subcooling of the liquid nitrogen increased with increase in the acceleration load. In the experiments the greatest subcooling was about 8°K, the greatest pressure $P = 2.5 \cdot 10^5$ N/m^2. We also carried out measurements at constant acceleration loads and various values of the subcooling, which depended on the thickness of the film on the heat-transfer surface.

Physicotechnical Institute of Low Temperatures, Academy of Sciences of the Ukrainian SSR, Kharkov.

Translated fron Inzhenerno-Fizicheskii Zhurnal, Vol. 53, No. 1, pp. 15-20, July, 1987. Original article submitted March 21, 1986.

0022-0841/87/5301-0749$12.50

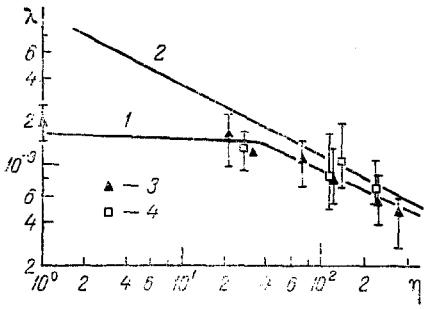

Fig. 1

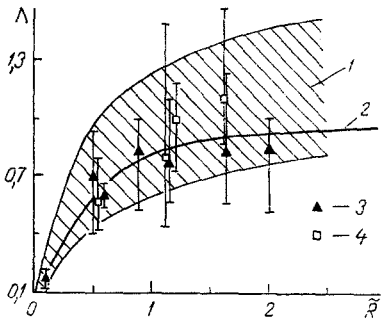

Fig. 2

Fig. 1. Wavelength λ (m) as a function of the acceleration load η: 1) λ_d for a cylindrical heater calculated from Eq. (1); 2) λ_{dF} for a flat heater calculated from Eq. (2); 3, 4) experimental data obtained by still and motion-picture photography.

Fig. 2. Wavelength Λ as a function of the dimensionless radius $\tilde{R}$: 1) data of [2]; 2) calculated from Eq. (5); 3, 4) see Fig. 1.

TABLE 1. Values of the Wavelength at Various Subcooling Levels

Acceleration load η	73	118	240	375
Subcooling ϑ, °K	0,5; 0,6; 1,0; 2,0; 3,2	0,7; 1,2; 2,5; 3,0	2,0; 3,1; 3,6	6,2; 7,8
Mean length $\lambda \cdot 10^3$, m	1,12; 1,14; 1,14; 0,9; 1,17	0,8; 0,8; 0,9; 0,85	0,6; 0,5; 0,6	0,5; 0,45

The experiments were carried out using photogrrahy at both increasing and decreasing heat loads. At constant values of the acceleration load and subcooling we took 25-30 photographs while recording the heat flux density corresponding to the frame. The linear scale on the still and motion-picture photographs was determined from the known distance between the heater and a control wire. The error of the measurements did not exceed $2 \cdot 10^{-4}$ m. In order to study the evolution of the boiling process, we made films at several values of the acceleration load and a constant heat flux $q = 4 \cdot 10^5$ W/m². The average filming speed was 4000 frames per second.

An analysis of the still photogrrphs and motion-picture projections of the nitrogen film boiling process showed that the effect of the centrifugal force field considerably modifies the hydrodynamic picture of the process of vapor phase formation and separation from the film. As the acceleration load increases, the bubble separation diameters and the wavelength at the film surface decrease considerably, while the bubble separation frequency increases.

At a constant acceleration load, as the heat flux increases a definite sequence of film boiling subregimes, differing with respect to the nature of the vapor separation from the film, is observed. In the regular regime ($q_{cr1,2} \leq q \lesssim 2.5\ q_{cr1}$) the vapor was separated from the film in the form of departing bubble. With gradual increase in the heat flux the size of the periodically departing bubbles increased somewhat, and at small acceleration loads (η = 1-22) coalescence of adjacent bubbles was observed. Then the intensified convective currents distorted the shape of the film and the bubbles and vapor "columns" were formed. In the nonregular regime ($q \gtrsim 2.5\ q_{cr1}$) vapor formations of various shapes and sizes separated from the film (in the form of "proturberances"). However, the periodicity of the nucleation sites on the heater itself was preserved and the distance between sites was equal to the corresponding wavelength. With increase in the acceleration load the change of film boiling subregimes took place at higher heat fluxes.

At $\eta \geq 72$ and sufficiently high heat fluxes single-loop circulatory convection [5], observable from the distortion of the trajectories of the ascending vapor formations, was established in the working space. The center of the convective eddy lay somewhat below the heat transfer surface, and on the latter there were intervals with descending and ascending flows.

Wavelength. The experimental values of the wavelength on the surface of the vapor film are shown in Fig. 1 as a function of η. We measured the distance between nearest crests (elevations) at the upper edge of the film in the regular film boiling regime and the distance between nucleation sites in the nonregular regime. At a constant acceleration load these values were equal. The experimental data are in satisfactory agreement with calculations based on the Lienhard–Wong equation [6] for the dominant wavelength for film boiling on cylindrical horizontal heaters

$$\lambda_d = 2\pi\sqrt{3}\Big/\sqrt{\frac{\eta g(\rho'-\rho'')}{\sigma}+\frac{1}{2R^2}}. \tag{1}$$

The correction for the thickness of the film was not taken into account in view of its small dimensions [2]. In Fig. 1 we have also plotted the theoretical curve for a flat heater [7]

$$\lambda_{dF} = 2\pi\sqrt{\frac{3\sigma}{\eta g(\rho'-\rho'')}}. \tag{2}$$

A comparison of the experimental data and the calculated curves shows that as the acceleration load increases the effect of the curvature of the heat transfer surface on the wavelength decreases.

The hydrodynamic film boiling characteristics of different liquids can conveniently be compared in dimensionless form using the parameters Λ and $\tilde{R}$ [2]:

$$\Lambda = \lambda/\lambda_{dF}, \tag{3}$$

where λ_{dF} is calculated from Eq. (2),

$$\tilde{R} = R\Big/\sqrt{\frac{\sigma}{\eta g(\rho'-\rho'')}}. \tag{4}$$

From (1) and (2) we obtain the expression

$$\Lambda = \sqrt{\frac{\tilde{R}^2}{\tilde{R}^2+0.5}}. \tag{5}$$

The experimental values of wavelengths, reduced to dimensionless form (Fig. 2), are in satisfactory agreement with the results of [2], in which the boiling of acetone, benzene and other liquids was investigated.

The considerable scatter of the Λ values observed under constant conditions ($\tilde{R}$ = const, η = const) confirms the conclusion drawn in [2] concerning the existence of a fairly broad spectrum of dominant wavelengths.

On the subcooling interval investigated the wavelength does not depend on the subcooling (see Table 1). However, an increase in the subcooling results in an extension of the heat fluxes at which the regular film boiling regime is observed.

Bubble Separation Diameter and Frequency. Analysis of the forces acting on a bubble in film boiling [8] makes it possible to obtain an expression for calculating the bubble separation diameter under the following assumptions: 1) the principal effect is that of the buoyancy force F_A and the surface tension forces F_σ; 2) the separating bubble is spherical; 3) the diameter of the bubble "neck" d is proportional to the wavelength λ_d (see diagram in Fig. 3)

$$d = k_1\lambda_d, \tag{6}$$

where $k_1 < 1$, λ_d is found from (1). This assumption takes into account the special character of film boiling on a cylindrical heater; 4) the diameter of the separated bubble D_d is proportional to the diameter of the bubble D_0 at the moment of loss of stability (when $F_A = F_\sigma$):

$$D_d = k_2 D_0. \tag{7}$$

With these assumptions taken into account, in film boiling the expression for the diameter of the separated bubble may be written in the form:

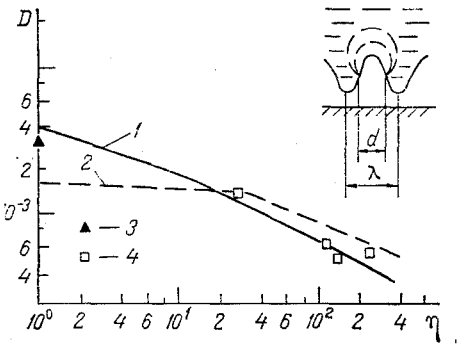

Fig. 3

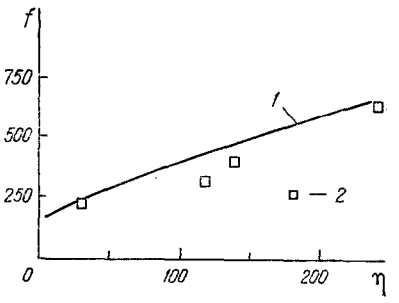

Fig. 4

Fig. 3. Bubble separation diameter D (m) as a function of acceleration load η: $q = 4 \cdot 10^5$ W/m²; 1) separation diameter calculated from Eq. (9); 2) wavelength on surface of film, Eq. (1); 3, 4) see Fig. 1.

Fig. 4. Bubble separation frequency f (1/sec) as a function of acceleration load η: 1) calculated from Eq. (10); 2) experimental data.

$$D_d = k_2 \sqrt[3]{\frac{6k_1\lambda_d\sigma}{g\eta(\rho' - \rho'')}}. \tag{8}$$

Correct to a proportionality factor equal to $k_2\sqrt[3]{k_1} = 1.7$, expression (8) gives a satisfactory description of the experimental $D_d(\eta)$ dependence (Fig. 3, curve 1).

On passage to the limit of film boiling on a flat plate (λ_d (1) → λ_{dF} (2)) expression (8) yields the proportional dependence

$$D_d = K\lambda_{dF}, \tag{9}$$

where K = 0.6 when $k_2\sqrt[3]{k_1} = 1.7$. A comparison of the graphs of $D_d(\eta)$ and $\lambda_d(\eta)$ (Fig. 3) shows that a tendency towards a proportional dependence of D_d on λ_d (curves almost parallel) is observed at $\eta > 40$, i.e., the effect of the curvature of the heat transfer surface dwindles. In experimental study [3] the bubble separation diameter was determined from Eq. (9) for K = 0.8 and in [6] for K = 0.5.

A theoretical expression for the bubble separation frequency was obtained from the equation for the angular frequency of the dominant wave ω_d [6]:

$$f_d = \frac{\omega_d}{2\pi} = 2\sqrt{\frac{\pi\sigma}{\lambda_d^3(\rho' + \rho'')}}. \tag{10}$$

The experimental values of the bubble separation frequency were found from the results of motion-picture photography: from the known speed we calculated the time T in which N (30-50) bubbles separated from a heater interval of length $L = 10^{-2}$ m. Knowing the wavelength for a given acceleration load, we found the number of waves on this interval. The mean rate of bubble separation from a single wave was calculated as

$$f = \frac{N\lambda}{TL}. \tag{11}$$

The experimental data obtained (Fig. 4) confirm the possibility of calculating the bubble separation from the film in accordance with Eq. (7).

In conclusion, we note that this investigation of the film boiling of liquid nitrogen in a centrifugal force field confirms the possibility of calculating the wavelength (1) and the bubble separation diameter (8) and frequency (10) for cryogenic liquids.

NOTATION

a, acceleration at heater level, m/sec²; D, bubble diameter, m; d, bubble "neck" diameter, m; F, force, N; f, bubble separation frequency, 1/sec; g, acceleration of gravity, m/sec²;

K and k, coefficients; L, length of the heater interval, m; N, number of bubbles; P, pressure, N/m^2; q, specific heat flux, W/m^2; R, heater radius, m; R, dimensionless radius; T, time, sec; $\eta = a/g$, acceleration load; θ, liquid subcooling at heater level, K; λ, wavelength, m; Λ, dimensionless wavelength; ρ, density, kg/m^3; σ, surface tension, N/m; ω, angular frequency, 1/sec. Subscripts: d, dominant wave; ', liquid; ", vapor; F, a plane heater; crl, transition from nucleate to film boiling; cr2, transition from film to nucleate boiling; A, buoyancy force; σ, surface tension force; and 0, moment of loss of stability.

LITERATURE CITED

1. R. J. Simoneau and K. J. Baumeister, Adv. Cryog. Eng., 16, 416-425 (1971).
2. J. H. Lienhard and K. Sun, Trans. Am. Soc. Mech. Eng. Ser. C, J. Heat Transfer, 92, No. 2 (1970).
3. M. Pomerantz, Trans. Am. Soc. Mech. Eng. Ser. C, J. Heat Transfer, 86, No. 2 (1964).
4. N. M. Levchenko, "Investigation of cryogenic liquid heat transfer in a centrifugal force field: Visualization. Onset of boiling. Boiling crises," Preprint, Physicotechnical Insitute of Low Temperatures, Academy of Sciences of the Ukrainian SSR, Kharkov (1986).
5. S. I. Sergeev, O. M. Popov, and I. P. Vishnev, Inzh.-Fiz. Zh., 46, No. 1, 100-107 (1984).
6. J. H. Lienhard and P. T. Y. Wong, Trans. Am. Soc. Mech. Eng. Ser. C, J. Heat Transfer, 86, No. 2 (1964).
7. R. Bellman and R. Pennington, Q. Appl. Math., 12, 151 (1954).
8. Yu. A. Kirichenko, Inzh.-Fiz. Zh., 25, No. 1, 5-13 (1973).

OPERATION OF A U-SHAPED THERMOSIPHON AT SMALL ANGLES OF INCLINATION

V. A. Krivonos

UDC 536.248.2

The effect of the volume of heat-transfer agent and the angles of inclination of the branches of a thermosiphon on its internal thermal resistance is determined.

Two-phase thermosiphons are being increasingly used in various branches of technology and this has found expression in the volume of experimental research [1-9].

In a number of cases it is necessary to use thermosiphons of complex configuration. Thus, in [8] a U-shaped thermosiphon with two straight tubes (branches), parallel to the horizontal and to each other, was considered. The charge of heat-transfer agent and the spatial arrangement of the branches were not varied during the experiments.

Our object was to determine experimentally the optimum charge of heat-transfer agent for a U-shaped thermosiphon and the effect on its operation of the angles of inclination of the thermosiphon as a whole and its individual branches.

The thermosiphon (Fig. 1) had the following geometric characteristics: outside diameter 16 mm, wall thickness 1.5 mm, total length 1250 mm, lengths of heating and cooling zones 195 and 600 mm, respectively; the thermosiphon material was copper and the heat-transfer agent was distilled water.

On the inner surface of the heating zone we formed a metric thread with a 1-mm pitch. The heating and cooling zones make up the two branches, which are arranged one above the other at an angle of up to 10°. This type of thermosiphon is intended for use in the heat-transfer devices of the cooling systems of radioelectronic assemblies. The thermometric measurements were made with Chromel–Copel thermocouples. The thermocouple emf was recorded by means of a KSP-4 potentiometer (accuracy class 0.25). The temperature of the heating zone was measured with four thermocouples. In the adiabatic part on the surface of the thermosiphon beneath the insulation in the steady-state operating regime the surface temperature was equal to the vapor temperature. This temperature was determined by the thermocouple at the point T_v. Along the length of the cooling zone the temperature was measured at seven uniformly spaced points. The heating zone was wrapped with one layer of mica paper, on which nichrome wire 1.0 mm in

A. V. Lykov Institute of Heat and Mass Transfer, Academy of Sciences of the Belorussian SSR, Minsk.

Translated from Inzhenerno-Fizicheskii Zhurnal, Vol. 53, No. 1, pp. 20-26, July, 1987. Original article submitted April 10, 1986.

0022-0841/87/5301-0753$12.50